ASSESSMENT OF RENEWABLE ENERGY SUPPLY FOR SHORE SIDE ELECTRICITY IN GREEN PORTS

Miral Michel [(1)i], Akram Soliman [(2)] and Ahmed S. Shehata [(1)i]

(1) Marine and Offshore Engineering, College of Engineering and Technology, Arab Academy for Science, Technology and Maritime Transport, Alexandria, Egypt, miral.michel@adj.aast.edu

(2) Construction and Building Engineering, College of Engineering and Technology, Arab Academy for Science, Technology and Maritime Transport, Alexandria, Egypt, akram_soliman@aast.edu

i) Corresponding authors: Ahmed S. Shehata, e-mail: a_samir@aast.edu
Miral Michel, e-mail: miral.michel@adj.aast.edu

Keywords: Green Port, Renewable Energy, Experimental Prototype, Energy Management, Wind Energy, Solar Energy.

1. **ABSTRACT:** Nations' economies have become considerably dependent on ports. Because of the concentration of harmful levels of pollution in and around ports, many countries started to take on the green port approach worldwide, which lowers the impact of ports and their operation on the environment given the wide interest in adapting renewable energy sources in ports for their electricity demands. Because the port is located inside the city borders of Alexandria, Egypt, there is noise, traffic, and air pollution. Based on the proposed "Green Port" development project, this study offers a plan to convert seaports into ecologically friendly ports. To determine how effective shoreside electricity is at reducing emissions, this paper estimates the percentage of pollution emitted by ships in the form of particulate matter and CO_2. This pollution could be reduced by using a hybrid renewable energy system that connects to the grid and has wind turbines and photovoltaic cells to power berthed ships. The process will be simulated using the energy management system and an experimental model of a solar-wind hybrid power system to demonstrate that wind turbines and photovoltaic solar energy can be sufficient to meet all the ships' energy needs in the port of Alexandria. The simulation's results, combined with data from an experimental prototype, demonstrate the economic viability of the integrated renewable energy system in the port of Alexandria. The simulation's small-scale components sufficiently provided a continuous power rating of roughly 51% of each one-megawatt load.

2. INTRODUCTION

Ports, worldwide, are of the main contributors to pollution but have been neglected by environmental initiatives and regulations while significant attention was given to ships, until recently, which can be seen in some of the European Commission's regulations and recommendations in 2005 and 2006 regarding the provision of shore electricity in ports near city limits. The European Union (EU) was the first to implement standard port regulations regarding energy efficiency, reduced power consumption and the use of green technology to reduce the carbon footprint of its ports since air pollution in port areas has become a problem of great importance during the last years [1]. The atmosphere in port areas is polluted not only by ordinary sources but also by ships and some specific harbor activities [2].

The usage of biomass-fired boilers in Koper port is one of how many ports throughout the world that employ various techniques to meet their energy needs and lessen their reliance on utility electricity. Enough wood debris was available at Slovenia's major terminal port of Koper to replace outdated boilers that used additional light fuel oil by producing biofuel for heating needs. Because biomass is a fuel that is CO_2 neutral, this consumption of 1742 MWh allowed the port to reduce 369 tons of CO_2 emissions annually and reduce cost by 98,000 € [3]. Additionally, the ports of Los Angeles and Long Beach employ electric rubber tire gantries, hybrid tugboats, and electric drayage vehicles [4]. It is clear that green ports do more than just use renewable energy sources; they also employ ways to lessen their reliance on fossil fuels and improve the overall energy efficiency of all of their equipment by integrating smart or micro grids, which guarantee power supply stability in favorable and unfavorable circumstances [5].

The German city of Hamburg and its port are well-known locations for encouraging the use of renewable energy. With an energy management policy that aligns with the smart city initiative, the port owns half of the city's 52.75 MW of wind turbines. In addition, the port has two 12 MW solar energy installations, which generate approximately 500 MWh of energy annually, and additional roof-top solar thermal energy installations for water heating, which add up to 56 MWh of energy savings annually [6]. All these methods reduce the needs of the port from the grid to about 120 MWh per year [7].

To encourage ecologically friendly shipping in Singapore, the Maritime and Port Authority of Singapore launched the "Maritime Singapore Green Initiative" in 2011. The goal of this project was to reduce greenhouse gas emissions from maritime transportation. Over the next five years, $100 million will be allocated to three main programmes: the Green Ship Programme, the Green Port Programme, and the Green Technology Programme. The Maritime and Port Authority of Singapore committed to funding the Maritime Singapore Green Initiative with up to $100 million throughout the next five years, starting on June 30, 2016, for example. Several energy-saving and CO_2-reducing initiatives were part of the 2009 Port of Singapore Authority's "Go Green" campaign. These included [8]:

(1) Using complete wall panels in workplace design, using natural lighting, installing motion sensors in rooms and hallways with little foot activity, allowing natural ventilation in restrooms surrounded by vegetation, and creating landscape buildings to offer cooling and lessen the effects of urban heat.

(2) Converting radioisotope thermoelectric generators (RTGs) to electrically powered E-RTGs.

(3) Fuel-saving devices should be installed to cut down on diesel usage.

(4) Hybrid hydraulic drive systems should be used to save fuel consumption by 20%.

Another example may be found in the port of Hong Kong, where the Hong Kong Economic Development and Labor Bureau states that the main goal of the Hong Kong Port (HKP) Master Plan 2020 is to develop a competitive and sustainable strategy for port development over a 20-year planning period. The entire ocean-container throughput in Hong Kong is expected to rise from 13.9 million twenty-foot equivalent units (TEUs) in 2002 to 31.87 million TEUs in 2020, with forecasts in HKP 2020 indicating that overall container traffic in Hong Kong will reach 40.2 million TEUs in 2020. To lower sulfur emissions, the Hong Kong government has supported several programs. In 2008, it mandated that all industry, including off-road vehicles, use ultra-low-sulfur diesel (ULSD) fuel, which burns cleaner than conventional diesel. The Hong Kong port operators, Hong Kong International Terminals (HIT), and Modern Terminals Ltd., have also switched from burning diesel fuel to using electricity to power their rubber-tired gantry cranes in 70% of HIT terminals. This resulted in savings of more than 120,000 kW annually. In the internal waters of Hong Kong and in the port's vicinity, vessel operators entering the port are required by the MARPOL VI agreement to burn fuels that release less than 2.5% sulfur [8].

3. AIM AND OBJECTIVES

Considering numerous limitations, this article examines the Alexandria port case study and the applicability of green port concepts, which include specific renewable energy technologies that are appropriate for implementation. Additionally, this study attempts to quantify the amounts of CO_2 and particulate matter that ships in Alexandria port emit, as well as investigate the possibility of using shoreside electricity to cut down on emissions by supplying the ships with power from a hybrid renewable energy system that includes grid-connected photovoltaics and wind turbines [9].

The energy management system and an experimental model of a solar-wind hybrid power system will be utilized in simulations to demonstrate that the hybrid system is capable of meeting all of the ships' energy needs while they are in port [10]. As for the system choice, the combined hybrid system was considered mainly for space constraints since solar energy on its own, or wind energy for that matter, would not be a sufficient approach [11]. This way each source will complement the temporary deficiencies of the other due to the limited space in the port and the fact that it has become well within one of the city's most populated areas. The software used for the simulation is HOMER with the data available for the port of Alexandria. Vertical axis wind turbines will be used in the design which give several advantages [12] since they can be easily packed in tighter spaces and require no change in the orientation when the wind changes direction which makes them able to make use of gusty winds, which are a common occurrence in Alexandria [13].

4. METHODOLOGY

4.1 Case Study

Alexandria Port occupies the leading position in the ports of Egypt regarding the volume of trade movement accounting for about 60% of Egypt's foreign, with history dating back to the founding of the city itself. Unfortunately, because it is situated inside city limits and firmly inside metropolitan regions, it is also one of the most polluted areas with significantly greater environmental impact.

The goal of this project is to present a thorough analysis of the port's circumstances and the effective application of green port principles. The port's coordinates are 31°12′16″ N 29°52′48″ E / 31.2045796° N 29.8800659° E. Its land area is 22.8 square kilometers.

4.2 Mathematical Formulations

The amount of energy that could be produced from solar and wind radiation can be calculated using a variety of techniques and mathematical models. In this part, examples of such models are given. They will be utilized as an input source for the data from the experimental device and to cross-check and validate the data collected by the simulation. While indeed the computer simulation is expected to be more accurate, this discrepancy between the two methods is expected to be negligible at best or minimal at worst. This will also highlight the important elements in these calculations.

The most important aspect is, naturally, the availability of such energy sources. Because they are most closely tied to the conditions in the port, the shore conditions are the study's focus. The Mediterranean Sea's beachfront experiences wind speeds that fall comfortably between 3.5 and 4 m/s. Egypt receives 2,400 hours of high intensity solar radiation each year, or 2,600 kWh/m², from the sun. As for wind power estimations, the wind power P_w (W) is presented in Eq. (1):

$$P_w = 0.5\ \rho_{air}\ A_S\ C_P\ v_w^{\ 3} \tag{1}$$

Where: the power coefficient is (C_P), wind speed (v_w) is in m/s, swept area (A_s) is in m², and air density (ρ_{air}) is 1.23 kg/m³. The power generated by a certain wind turbine can be determined using this general equation [14]. It describes the theoretical power output from the motion of air, and then applies the turbine's efficiency (C_P). Most manufacturers grade their turbines based on how much power they can generate safely at a specific wind speed, which is typically selected between 10.5 and 16 m/s.
The formula shows the elements that are crucial to a wind turbine's performance. With an exponent of 3, the wind speed, v_w, indicates that even a slight increase in wind speed yields a significant gain in power. Because larger towers can access higher wind speeds, they boost the productivity of any wind turbine. Since the rotor of the turbine is the component that harnesses wind energy, the rotor swept area, or A_S, is significant. Thus, the rotor's capacity to capture energy increases with its size.
Elevation and air temperature have a small impact on the density of air, ρ_{air}. The standard conditions of 15°C at sea level are used to determine the ratings for wind turbines [15]. Naturally, a vertical turbine uses the elevation of its geometric centre rather than a central "hub." Also, the swept area in the calculations will be replaced by the vertical turbines' cross-sectional area. These alterations will be used both in the simulation and other calculations [16].

For the calculation regarding the experimental model, another way is used to calculate its power output. This is done since efficiency (C_P) is not a known value yet, and it cannot be compared to similar commercial turbines due to difference in scale. Therefore, the equation used for calculating the power output will be Eq. (2):

$$P_w = 2\ \pi\ \frac{N}{60}\ T \tag{2}$$

Where (T) is the generated torque and (N) is the turbine's revolution per minute. The efficiency of the turbine can then be found by dividing this power by the theoretical power output that was determined using the first equation.

Because the loss factor, which defaults at 0.75, ranges from 0.5 to 0.9, solar panels are extremely efficient [17]. Under all conditions, all of these formulations are roughly comparable and nearly related [18], as demonstrated by Eq. (3):

$$E = 365\ P_k\ r_p\ H_h \tag{3}$$

Where (P_k) is the maximum power of the installed equipment in kW, (r_p) is the reduction factor (-) or system performance ratio, (E) is the yearly power generation potential in kWh, and (H_h) is the worldwide daily or annual average value of radiation in Wh.

Eq. (4) illustrates a different proposed calculation that is based on the yearly generation of electricity [19]:

$$E_{out} = A_e\ E_e\ G \tag{4}$$

Where (A_e) is the total area (the pure active area) of solar cells in meters, (E_e) is the efficiency coefficient for power conversion for each PV, and (G) is the yearly global irradiation in Wh/m^2. The annual electrical output is expressed in kWh.

Measurements and results from the experimental model are gathered over several days at various times of the day using a data logger. Furthermore, as demonstrated by the appliances, manual recording of volt and ampere is done using a multi-meter. Eq. (5) computes the electrical powers as follows:

$$P_{electrical} = V\ I \tag{5}$$

Where (V) is the output voltage in volts, (I) is the output current in Amps, and ($P_{electrical}$) is the yearly electricity production in Watts.

4.3 Experimental Setup

This experiment is carried out to provide an indication of the efficacy of a hybrid power unit that might serve as a model for the green power system proposed in this study for the port of Alexandria, or any port with comparable weather and source circumstances.

As depicted in Figs. (1a) and (1b), the prototype utilized to carry out this experiment is made up of a chassis that supports a PV cell and a twist vertical axis turbine. They come with a torque-speed meter that measures torque and provides power and rotation speed information.

Figure 1: The Hybrid Power Unit, (a) Front View and (b) Side View

The wind tunnel unit, shown in Fig. (2), which was utilized consists of a convergent section, straightener section, 12" x 12" x 34" I.D. test section, divergent section and fan section. The 27" tube axial fan wheel has a top speed of 13,362 FPM at 1800 RPM. The fan is driven by a 15 HP three-phase motor controlled by a variable frequency drive with keypad speed control 0 – 60Hz. A pitot tube positioner can accurately position the pitot tube to within 0.02 cm of its vertical linear position and 0.2° of its angular position by use of vernier scales. The positioner has a maximum linear range of 25 cm and rotary range of 360°. The mobile support frame is constructed of 2" square mechanical tubing with trusses and cross members to support the wind tunnel and worktable. The electrical control box consists of a 3-pole main circuit breaker with associated pilot light, accessory power receptacle, and a 10 ft. 5/c power cord with cord rack.

Figure 2: Wind Tunnel Unit

The setup is shown in Figs. (3a) and (3b). Wind speeds of 3.5, 4, 5, 6, 7, 8, and 9 m/s were examined while imposing various loads on the turbine [20].

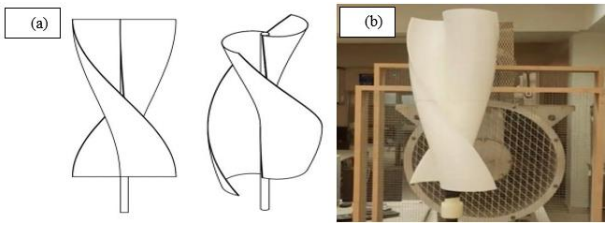

Figure 3: Twist vertical axis turbine, (a) Turbine Design and (b) Wind Tunnel

The device was also placed outdoors to test the solar panel performance as shown in Fig. (4a) and (4b).

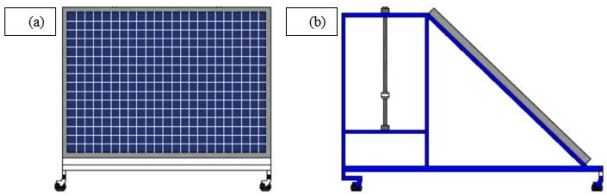

Figure 4: The PV Cell, (a) Front View and (b) Side View

Several voltage and current readings were taken at different times throughout the day. A commercial grade solar panel of power rating of 80 W was used, which is expected to produce about 0.08 kWh in normal operational conditions. It has a footprint of 0.578 m^2 and it was fixed at an angle of 45 degrees. The model has a maximum working voltage of 17.75 V and a maximum power current of 4.5 A.

Along with the panel, a 5A solar charger/controller is used. A dynamic PLC568 rotating torque sensor is used to detect the rotation torque of the turbine. Its working principles are as follows:

(1) Torque measurement after amplification, the strain signal is transformed into a frequency signal, proportional to the torque.

(2) Measurement of rotating speed, the rotating speed signal is converted into impulse signal through the optical coupling and processing circuit, and the rotating equipment outputs 60 pulses per revolution.

4.4 Modelling Software

HOMER Energy™ software is used to simulate the hybrid power system and give analytical data regarding the plausibility of applying renewable energy hybrid systems and its economic feasibility. Several electrical equipment types, such as generators, converters, batteries, AC (alternating current) and DC (direct current) loads, operate together under various limitations and climatic conditions in this

software simulation of an electrical grid. All the model's constituent parts are considered by the simulation approach for brief time fluctuations at the minute scale. Using satellite weather data, "HOMER Energy" software additionally yields solar radiation information based on the installation location's geographic coordinates. An electric model was developed in the simulation program to quantify energy from renewable sources and possible reductions in CO_2 emissions using combinations of 250 kW to 1000 kW solar systems and 100 to 800 kW wind turbines. To simulate the various sizing alternatives and climatic circumstances, a lean AC bus model is employed. Since accurate data regarding power needs and consumption were hard to come by and the authorities would not share such data with the public, the simulation was set to provide the needs of a constant load of 1 MW, making it a dimensionless reference for the port of Alexandria. This allows the data to be used to assess projects of varying scales. When calculating the reduction in CO_2 emissions from the power plant, HOMER Energy uses an emission factor of 680 g/kWh, while the ships use an EF of 700 g/kWh. The software used to determine the decrease of PM used an energy factor of 0.3 g/kWh for the ships and 0.091 g/kWh for the power plant. The standard utilized in the software was 1 kWh, which is equivalent to 3.6 MJ of energy, as illustrated in Fig. (5).

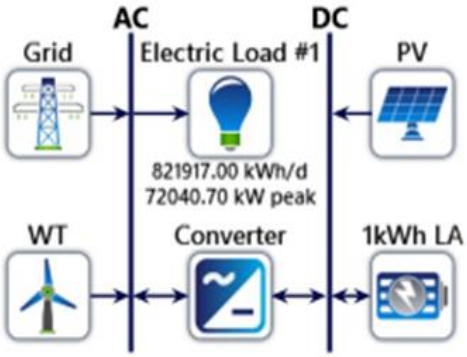

Figure 5: Schematic Diagram of the Relations Between Grid and Renewable Application.

5. RESULTS AND DISCUSSION

This section's analysis is made up of two significant studies. First, a hybrid system comprising a PV solar panel and a hybrid vertical axis wind turbine is the subject of an experimental investigation. This paradigm is used in the context of Alexandria Port. Depending on performance, the impact of various free stream velocities on the hybrid turbine is examined. In the meantime, tests are conducted on the solar PV panel and its performance is examined in relation to combining it with the wind turbine. After that, the simulations are carried out numerically using HOMER software. To determine the hybrid system's effectiveness, four scenarios are examined. A grid with a solar system, a grid with a wind system, and a grid with a hybrid solar-wind system are all studied and analyzed in these scenarios. For comparative study, the four cases are utilized.

5.1 Experimental Results

Wind Turbine Configuration: The turbine was tested at different air velocities with different load conditions at each air speed. Table 1 contains these readings as follows.

Table 1. Wind turbine results at different air velocities, with different load conditions

V (m/s)	*Load (%)*	*Rotational Speed (rpm)*	*Torque (N.m)*	*Power (W)*
3	0	9	0.08	0.11
3.5	0	26	0.06	0.16
	10	16	0.07	0.12
4	0	51	0.06	0.32
	10	18	0.08	0.15
5	0	115	0.05	0.6
	10	18	0.08	0.15
6	0	255	0.05	1.34
	10	150	0.1	1.57
	20	100	0.12	1.26
	30	35	0.1	0.37
7	0	305	0.04	1.28
	10	160	0.08	1.34
	20	80	0.1	0.84
	30	60	0.12	0.75
8	10	160	0.09	1.51
	20	105	0.12	1.32
	30	95	0.13	1.29
	40	65	0.15	1.02
9	10	190	0.18	3.58
	20	110	0.22	2.53
	30	80	0.23	1.93
	40	70	0.25	1.83

The data obtained from the wind tunnel tests were at different air velocities.

At each velocity, the turbine was tested under several loads numbered from 0% to 40%, where 0% indicates no load condition. With the load 10% giving the highest power results. Thus, the coming analysis and calculations for the turbine will consider the results of the test at various wind speeds and the loading condition 10% as shown in Table 2. This shows a tendency towards a better performance at the range of air speeds close to the 6 m/s mark.

Table 2. Wind turbine efficiency at loading condition 10%

V (m/s)	*Rotational Speed (rpm)*	*Torque (N.m)*	*Power (W)*	*Efficiency (%)*
3.5	16	0.07	0.117	4.5
4	18	0.08	0.151	3.9
5	75	0.08	0.63	8.3
6	150	0.1	1.57	12

7	160	0.08	1.34	6.4
8	105	0.09	1.508	4.8
9	190	0.18	3.581	8.1

As seen in Figs. (6a) and (6b), efficiency decreases at air speeds greater than 6 m/s before increasing again after 9 m/s. Further speeds were deemed unnecessary for testing, as such wind velocities are rarely reported in this region.

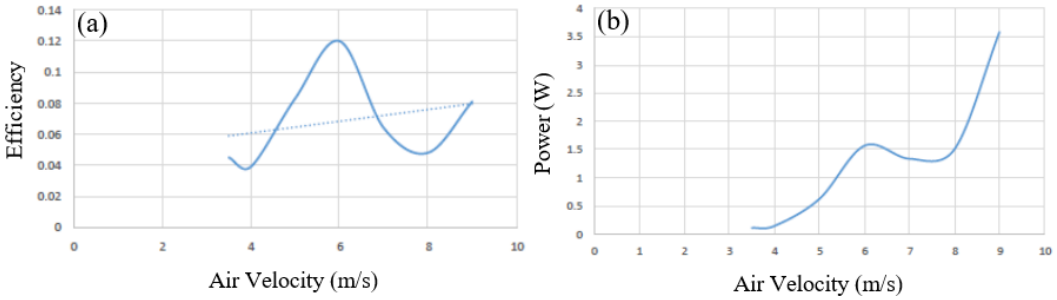

Figure 6: Wind Turbine Performance at a Range of Air Speeds vs a) Efficiency and b) Power

Solar Panel Data: The data from the solar panel was taken hourly on a relatively sunny day. Voltage and current were measured, then the power was calculated. Table 3 summarizes these readings.

Table 3. The range of power rating throughout the day

Time of Day	*Temperature (°C)*	*Humidity (%)*	*Voltage (V)*	*Current (A)*	*Power (W)*
9 :00 AM	14	68	20.75	3.48	72.13
10 :00 AM	17	60	21.37	3.63	77.64
11 :00 AM	19	60	21.66	3.94	85.36
12 :00 PM	21	50	21.7	3.96	86
01 :00 PM	22	52	21.55	3.88	83.72
02 :00 PM	19	55	21.5	3.5	75.25
03 :00 PM	19	58	21.63	3.85	83.26

As for the output of the solar panel, it performed within the range of its power rating throughout the day. This is also noted to be the case under different temperatures and humidity levels. The power did not fall much below the rated power of 80 W, with the minimum reading of 72 W. It is noted, however, that these readings were taken on a rather sunny day, thus, these readings do not account for the performance of the unit in shades. This gives the unit an average power generation of about 80 W during the day. This indicates an average of 138.5 W per 1 m^2 of area for this type of solar panel.

5.2 Simulation Software

The system can provide 51% of the demand, reducing the dependence on the grid down to only 49% of the demand. Notably, this simulation result is yielded using very small-scale equipment in the

simulation model; using larger-scale equipment will yield far better results. The simulation report gives more detailed information about the economics of the project and the several charts give an indication of the overall performance. As for the emission reduction, the program has calculated the expected reduction in CO_2, NO_x, SO_2, and particulate matter generated.

These pollutants are released into the atmosphere because of the following processes: the generator(s) producing electricity, the boiler producing thermal energy, and the consumer using grid electricity. Given that both boilers and generators use fuel with established characteristics, HOMER simulates their emissions similarly. It uses a slightly altered grid model.

Table 4 shows the reduction in the aforementioned quantities in kilograms per year. Slightly less than 3000 metric tons carbon dioxide emissions are produced per year with sulfur dioxide reduced by 12 tons each year and just shy of 6 tons less nitrogen oxides every year.

Table 4. Emission reduction values

Quantity	*Value (kg/year)*
Carbon dioxide	2,991,444
Carbon monoxide	0
Unburned hydrocarbons	0
Particulate matter	396
Sulfur dioxide	12,054
Nitrogen oxides	5,895

Table 5 shows various combinations of energy sources that were previously used, and their cost compared to the cost of the proposed system.

Table 5. Comparison between previous studies and the proposed system

Reference	*System*	*Cost of Energy ($/kWh)*
Baneshi, M. and F. Hadianfard [21] in Iran	PV/wind turbine/battery	0.093 – 0.126
	PV/wind turbine/grid	0.057 – 0.084
Shahzad, M. K., et al. [22] in Pakistan	PV/biogas-fuelled generator/batteries	0.036
Alwaeli, A. [23] in Oman	PV/batteries	0.467
	Wind turbine/batteries	5.184
	Diesel generator	0.567
	PV/wind turbine/batteries	0.38
Proposed System in Egypt	Grid	0.14
	Grid/PV	0.095
	Grid/wind turbine	0.087
	Grid/wind turbine/PV	0.08

By default, the program considers any demands to be met by such means, then calculates the reduction in emissions based on the amount of electric power that is no longer provided by these sources in the cases of generators, boilers, and reformers. HOMER calculates the emissions factor (kg of pollutant emitted per unit of fuel consumed) for each pollutant before modeling the power system. Following the simulation, the emissions factor is multiplied by the total annual fuel use to get the

pollutant's annual emissions. HOMER determines the emissions factors for the two remaining pollutants, carbon dioxide and sulfur dioxide, using these values for four of the six pollutants: carbon monoxide, unburned hydrocarbons, particulate matter, and nitrogen oxides, as well as the fuel's carbon and sulfur content. To simulate a system that is connected to the grid, HOMER determines the net grid purchases, which are determined by deducting the total grid sales from the total grid purchases. Emission factors (in g/kWh) for each pollutant are multiplied by net grid purchases (kWh) in HOMER to determine the emissions of each pollutant related to these purchases. The net grid purchases, and the emissions of each pollutant associated to the grid will be negative if the system sells more electricity to the grid than it purchases from it during the course of the year.

6. CONCLUSION

In conclusion, the data from the experimental prototype and the simulation both support the viability of incorporating renewable energy sources into the Alexandria port's power supply system. Although the precise port load estimates are not publicly available, the simulation's small-scale components were able to consistently and profitably supply a continuous power rating of roughly 51% of a megawatt load, suggesting that if industrial-grade equipment with the same footprint were employed, a sizable portion of the port's power demands could be met. As the simulation results suggest, the use of solar panels of 350 kW rating, which is about 1000 square meter footprint, not a large space relative to the port and the roof tops of the various buildings and hangars of the port, can accommodate many multiples of that space requirement. In addition, this is done using a basic solar panel of about one square meter with a rating of 355 watts. The hybrid design similar to that of the prototype can save a lot of space since both power systems occupy the same space. The experimental prototype shows promise regarding the overall efficiency and plausibility of the system.

7. REFERENCES

[1] A. M. Kotrikla, T. Lilas, and N. Nikitakos, "Abatement of air pollution at an aegean island port utilizing shore side electricity and renewable energy," *Marine Policy*, vol. 75, pp. 238-248, 02/01 2017, doi: 10.1016/j.marpol.2016.01.026.

[2] N. Kozarev, S. Stoyanov, and N. Ilieva, "AIR POLLUTION IN PORT AREAS," 11/30 2023.

[3] B. Pavlic, F. Cepak, B. Sucic, M. Peckaj, and B. Kandus, "Sustainable port infrastructure, practical implementation of the green port concept," *Thermal Science*, vol. 18, pp. 935-948, 01/01 2014, doi: 10.2298/TSCI1403935P.

[4] B. Quinn, "Walmarts sustainable supply chain," *Pollution Engineering*, vol. 41, 09/01 2009.

[5] I. Kotowska, "Policies Applied by Seaport Authorities to Create Sustainable Development in Port Cities," *Transportation Research Procedia*, vol. 16, pp. 236-243, 2016/01/01/ 2016, doi: https://doi.org/10.1016/j.trpro.2016.11.023.

[6] D. Han, Y. G. Heo, N. J. Choi, S. H. Nam, K. H. Choi, and K. C. Kim, "Design, Fabrication, and Performance Test of a 100-W Helical-Blade Vertical-Axis Wind Turbine at Low Tip-Speed Ratio," *Energies*, vol. 11, no. 6, doi: 10.3390/en11061517.

[7] M. Acciaro, H. Ghiara, and M. I. Cusano, "Energy management in seaports: A new role for port authorities," *Energy Policy*, vol. 71, pp. 4-12, 2014/08/01/ 2014, doi: https://doi.org/10.1016/j.enpol.2014.04.013.

[8] Y.-C. Yang and W.-M. Chang, "Impacts of electric rubber-tired gantries on green port performance," *Research in Transportation Business & Management*, vol. 8, pp. 67–76, 10/01 2013, doi: 10.1016/j.rtbm.2013.04.002.

[9] J. Zhu, L. Jiang, and H. Zhao, "Effect of wind fluctuating on self-starting aerodynamics characteristics of VAWT," *Journal of Central South University*, vol. 23, pp. 2075-2082, 08/01 2016, doi: 10.1007/s11771-016-3263-1.

[10] A. Ahmedov, "Investigation of the Performance of a Hybrid Wind Turbine Darrieus-Savonius, PhD Thesis," 2016.

[11] J. Akwa, H. Vielmo, and A. Petry, "A review on the performance of Savonius wind turbines," *Renewable and Sustainable Energy Reviews*, vol. 16, pp. 3054–3064, 06/01 2012, doi: 10.1016/j.rser.2012.02.056.

[12] N. H. Mahmoud, A. A. El-Haroun, E. Wahba, and M. H. Nasef, "An experimental study on improvement of Savonius rotor performance," *Alexandria Engineering Journal*, vol. 51, no. 1, pp. 19-25, 2012/03/01/ 2012, doi: https://doi.org/10.1016/j.aej.2012.07.003.

[13] M. Islam, D. S. K. Ting, and A. Fartaj, "Aerodynamic models for Darrieus-type straight-bladed vertical axis wind turbines," *Renewable and Sustainable Energy Reviews*, vol. 12, no. 4, pp. 1087-1109, 2008/05/01/ 2008, doi: https://doi.org/10.1016/j.rser.2006.10.023.

[14] N. Willard, "Efficiency Investigation of a Helical Turbine for Harvesting Wind Energy," Master of Science, Mechanical and Industrial Engineering, Northeastern University, Boston, Massachusetts : Northeastern University, 2011. [Online]. Available: https://repository.library.northeastern.edu/files/neu:1671/fulltext.pdf

[15] W. E. Development. "How to calculate power output of wind." Windpower Engineering & Development. https://www.windpowerengineering.com/calculate-wind-power-output/ (accessed.

[16] J. Khan, G. Bhuyan, M. T. Iqbal, and J. Quaicoe, "Hydrokinetic Energy Conversion Systems and Assessment of Horizontal and Vertical Axis Turbines for River and Tidal Applications: A Technology Status Review," *Applied Energy*, vol. 86, pp. 1823-1835, 10/01 2009, doi: 10.1016/j.apenergy.2009.02.017.

[17] C. Carl, "Calculating solar photovoltaic potential on residential rooftops in Kailua Kona, Hawaii," 2014.

[18] F. Wang *et al.*, "Image phase shift invariance based cloud motion displacement vector calculation method for ultra-short-term solar PV power forecasting," *Energy Conversion and Management*, vol. 157, pp. 123-135, 02/01 2018, doi: 10.1016/j.enconman.2017.11.080.

[19] D. Wang, T. Qi, Y. Wang, J. Fan, Y. Wang, and H. Du, "A method for evaluating both shading and power generation effects of rooftop solar PV panels for different climate zones of China," *Solar Energy*, vol. 205, pp. 432-445, 07/01 2020, doi: 10.1016/j.solener.2020.05.009.

[20] R. E. Sheldahl, B. F. Blackwell, and L. V. Feltz, "Wind tunnel performance data for two- and three-bucket Savonius rotors," *Journal of Energy*, vol. 2, pp. 160-164, 1978.

[21] M. Baneshi and F. Hadianfard, "Techno-economic feasibility of hybrid diesel/PV/wind/battery electricity generation systems for non-residential large electricity consumers under southern Iran climate conditions," *Energy Conversion and Management*, vol. 127, pp. 233-244, 2016/11/01/ 2016, doi: https://doi.org/10.1016/j.enconman.2016.09.008.

[22] M. K. Shahzad, A. Zahid, T. ur Rashid, M. A. Rehan, M. Ali, and M. Ahmad, "Techno-economic feasibility analysis of a solar-biomass off grid system for the electrification of remote rural areas in Pakistan using HOMER software," *Renewable Energy*, vol. 106, pp. 264-273, 2017/06/01/ 2017, doi: https://doi.org/10.1016/j.renene.2017.01.033.

[23] A. Alwaeli, "Optimal Sizing of a Hybrid System of Renewable Energy for Lighting Street in Salalah-Oman using Homer software," *International Journal of Scientific Engineering and Applied Science (IJSEAS) – Volume-2, Issue-5,May 2016*, vol. ISSN:, pp. 157-164, 05/05 2016.